JOURNAL OF MATERIALS SCIENCE 9 (1974) 1171–1182

The application of self adjusting interfaces to the design of fibrous composites

J. G. MORLEY, R. S. MILLMAN
Wolfson Institute of Interfacial Technology, University of Nottingham, UK

In the case of orthodox fibre composite materials the mechanical properties of the interfaces are fixed at an almost constant level by a choice of materials and manufacturing techniques. In such systems semi-continuous reinforcing elements fail when the tensile strain in the composite becomes comparable with the failing strain of the fibres. It is shown that the reinforcing elements can be prevented from failing, whatever the tensile strain in the composite material, if the shear strength of the interface between the reinforcing elements and the rest of the composite structure is self adjusting and is reduced locally as the local tensile stress carried by a reinforcing element increases. The characteristics of experimental reinforcing elements possessing these features have been investigated and the properties of composites utilizing such fibres are discussed.

1. Introduction

In orthodox reinforced composite materials the fibres are usually strong, stiff and brittle and serve to stiffen and strengthen the matrix, primarily when the loads are applied in the direction of fibre alignment. In order that this may be achieved there must be some means of stress transfer between matrix and fibre across the fibre matrix interface. (For a discussion of this see, for example, [1].) Stress transfer can take place as a result of:

(a) differential longitudinal elastic deformation between fibre and matrix;

(b) frictional contact between fibre and matrix;

(c) plastic deformation in shear of the matrix near the interface (where the matrix is a ductile metal).

In reinforced polymers the stress transfer occurs normally by a combination of (a) and (b) [2, 3] whereas in fibre reinforced metals stress transfer is normally achieved through a combination of (a) and (c). In both cases the maximum value of shear stress transfer between individual fibres and the matrix is limited to a value which is set either by frictional effects (following debonding of the interface), or by the yield strength in shear of the matrix (if the matrix is deformable). In both conditions the shear strength of the interface is usually considered essentially constant over the stress transfer length of the fibre so that, to a first approximation, the tensile stress carried by the fibre can be regarded as increasing uniformly from the free end at a rate governed by the effective strength in shear of the interface. When the fibre is cylindrical

$$\sigma_x = \frac{2\tau x}{r} \tag{1}$$

where σ_x is the tensile stress carried by the fibre at a distance x from the free end, τ is the effective shear strength of the interface and r is the radius of the fibre. It follows from Equation 1 that if the fibre has a length greater than a critical length l_c where

$$l_c = \sigma_{ult} \frac{r}{\tau} \tag{2}$$

and σ_{ult} is the ultimate breaking stress of the fibres, the fibre will break if sufficient tensile strain is applied to the composite [4]. If the fibres have a high aspect ratio the composite failing strain will be similar to the failing strain of the fibres themselves. In the case of simple fibre composites containing an appreciable volume fraction of semi-continuous, strong, brittle fibres ($V > V_{crit}$) the failing strain of the composite is, therefore, controlled primarily by the failing strain of the fibres which, for materials of technological interest, is about 1%. If, however, τ can be made a function of fibre

tensile stress σ so that τ diminishes as σ increases, falling to zero before σ reaches σ_{ult}, the fibre tensile stress can never reach σ_{ult} whatever the fibre length and whatever the longitudinal displacement of the matrix with respect to it.

If we assume a linear relationship between the shear strength of the interface and the tensile stress carried by the fibre we have

$$\tau_\sigma = \tau_0 - K\sigma \tag{3}$$

where τ_σ is the strength in shear of the interface when the local stress carried by the reinforcing element is σ and τ_0 is the strength in shear of the interface when the local fibre tensile stress is zero.

Since $\tau_\sigma = 0$ when $\sigma = \sigma_{max}$

$$K = \frac{\tau_0}{\sigma_{max}}. \tag{4}$$

The rate of change of tensile stress carried by a cylindrical reinforcing element with increasing distance x from the free end is given by

$$\frac{d\sigma}{dx} = \frac{2\tau_\sigma}{r}$$

$$\frac{d\sigma}{dx} = \frac{2}{r}(\tau_0 - K\sigma)$$

or

$$\frac{d\sigma}{dx} + \frac{2\tau_0\sigma}{r\sigma_{max}} = \frac{2\tau_0}{r} \tag{5}$$

from which we have

$$\sigma_x = \sigma_{max}\,[1 - \exp(-2\tau_0 x/\sigma_{max} r)]. \tag{6}$$

It follows from Equation 6 that in a system of this type the tensile stress carried by the reinforcing element will increase with increasing distance along the fibre and approach the limiting value σ_{max} asymptotically.

There are some advantages in providing an interface of this type between the core and the sheath of a two part (duplex) reinforcing element [5]. In such an arrangement the core and sheath are effectively locked together and behave as a homogeneous solid reinforcing rod until the interfacial frictional forces become low enough to permit differential movement between core and sheath. When the sheath element fails in tension the load carried locally is reduced by an amount equal to the contribution of the sheath before failure, the core element, however, continues to carry a tensile stress up to the limiting value σ_{max}. If failure of the sheath element occurs while the stress carried by the core is less than σ_{max} the crack bridging core fibre can carry an increasing tensile stress with increasing tensile deformation of the composite up to the limiting value σ_{max}. This increased load is supported by an increasing elastic extension in the bridging fibre. Since the shear strength of the fibre matrix interface falls as the local fibre tensile load increases, the effective length of the bridging fibre undergoing elastic extension also increases. Eventually the stress distribution along the core fibre reaches the condition described in Equation 6 and further extension of the composite structure results in the core fibre being pulled bodily through the sheath against frictional forces.

2. An experimental duplex fibre system with self adjusting variable shear strength interface

2.1. Initial observations

2.1.1. Core element in tension

One method of producing a variable shear strength interface between a core and sheath is to have the core in the form of a convoluted spring pressing against the inside of a tubular sheath. The convolutions in such a system may be either helical or in a single plane, but in both cases the convolutions must be constrained by the walls of the tube so that a frictional force is generated between the core and sheath. It can be seen from geometrical considerations that when a tensile load is applied to an unconstrained convoluted core, the amplitude of the convolutions will be reduced so that when a tensile load is applied to a convoluted wire, initially constrained by the tube, there is a consequent reduction in friction across the interface. When the lateral dimensions of the core under load become the same as the internal dimensions of the tube the frictional forces are reduced almost to zero. This condition is the basic requirement of a variable shear strength interface.

Experimental reinforcing elements have been constructed, as described below, using convoluted piano wire or stainless steel wire contained within stainless steel hypodermic tubes. A length of wire was taken rather more than twice the length of the required duplex element. About half the length of this wire was closely wound onto a mandrel and then stretched to form an elongated helix with an external diameter greater than the i.d. of the tube. The straight section of the wire was then pushed

through the tube enabling the convoluted section to be pulled in after it. When a core wire is pulled into a tube initially, the interfacial contact area is small but the frictional interaction is very large, this means that the "pull-in" load is initially zero and rises rapidly as the first convolutions are pulled into the tube. As an increasing length of wire is pulled into the tube, the stress in the leading section of the core increases so that it makes a progressively smaller contribution to the frictional interaction. As a result of this, the rate of increase of "pull-in" load begins to diminish and finally approaches a limiting value. This limiting load is that which would be required to reduce the diameter of an unconstrained helix to that of the internal diameter of the tube. The stress distribution along the convoluted wire is described by Equation 6 and rises from zero at the point where the unstressed wire enters the tube to a value σ_x corresponding to the length x inserted in the tube. According to the simple theory the same stress distribution is obtained as the wire is being drawn into or out of the tube. The stress level σ_{max} is, therefore, approached asymptotically as an increasing length of convoluted wire is contained within the tube.

Initial experiments to investigate the characteristics of duplex reinforcing elements were carried out using wire and tube as shown below. The core elements were produced by winding the wire on a 1.03 mm diameter mandrel and prestressing with a load of 5.0 kg.

	Core	Sheath
Material	Stainless steel wire	Stainless steel hypodermic tube
Manufacturer	Stainless Steel Wire Co, Sheffield	Accles and Pollock, Oldbury, Birmingham
Outside diameter (D) (mm)	0.26	0.718
Inside diameter ($2x$) (mm)	—	0.419
Free amplitude (a) (mm)	0.507	—
Free wavelength (λ) (mm)	4.73	—

One end of the core wire was then suspended from the load cell of a table model Instron testing machine and a weight, W, was applied to the other (see Fig. 1). A 10 cm length of hypodermic tube was then pulled down over the core wire and the load, F, measured by the load cell was recorded. The experiment was repeated with various tensile loads applied to the wire. If it is assumed that the load carried by the wire

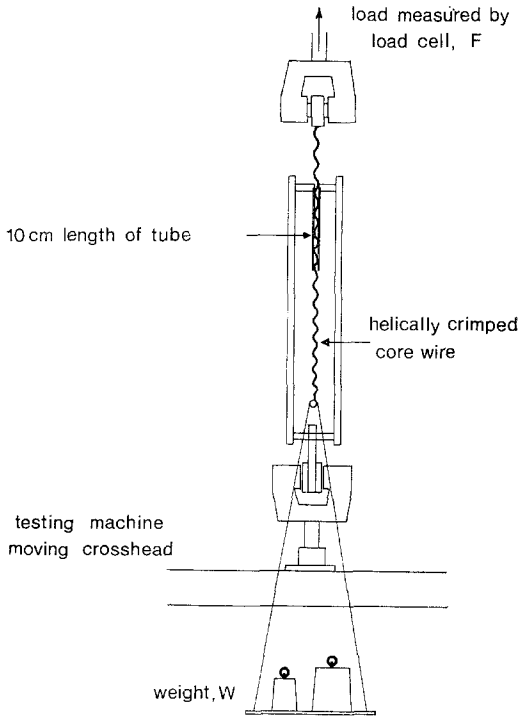

Figure 1 General arrangement of equipment used for "pull through" experiments.

increases linearly from W at one end to F at the other, the average tensile load on the wire is $W + (F - W)/2$ while the "pull through" load is $F - W$. By applying varying tensile loads to the wire, a curve of "pull through" load versus average tensile load was obtained (see Fig. 2). This curve, which can be seen to approximate to a straight line, was then produced to intercept the axes, from which were obtained values of τ_0, the shear strength of the interface under zero tensile load in the core, and L_{max}, the load necessary to debond the wire completely. The theoretical stress distribution along the core wire as it is pulled through the tube was then calculated by substituting these values into Equation 6. This curve labelled "uncorrected" is shown in Fig. 3. The experimental values of the loads required to pull the wire into and out of a long length of tube were then obtained for various lengths of core element in frictional contact with the tube and these are also shown in Fig. 3. In fact the effective average tensile load on the wire was not $W + (F - W)/2$ because the load does not vary linearly from W to F as assumed initially, but takes the form of a segment of an exponential curve. Using the "uncorrected" stress distribu-

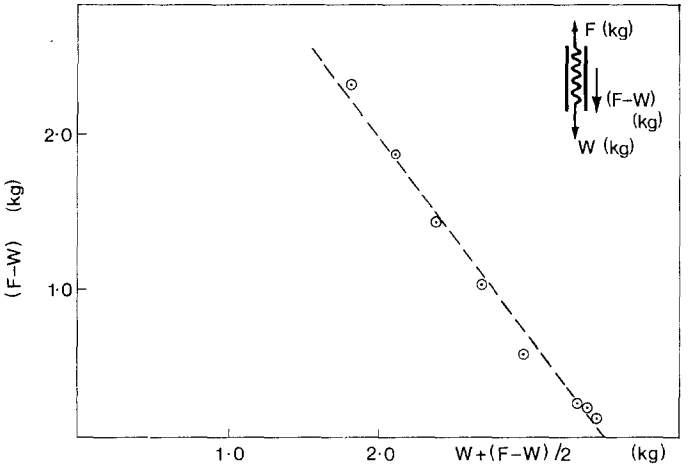

Figure 2 Relationship between "pull through" load $(F - W)$ and nominal tensile load $W + (F - W)/2$ applied to the core wire.

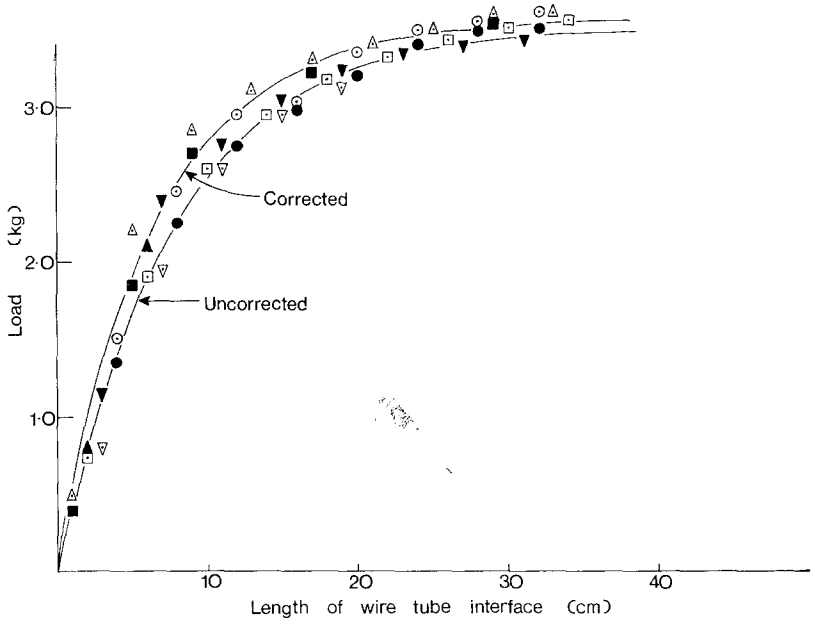

Figure 3 Experimental values of loads required to displace various lengths of convoluted wires within a tube, compared with calculated values.

tion curve a more accurate value of the true effective average load on the wire was obtained graphically and this was then resubstituted into Equation 6 and a second theoretical stress distribution was calculated and plotted – this is shown in Fig. 3 labelled "corrected". The correction procedure was not repeated since the correction factors became negligibly small in comparison with the experimental errors after the first computation.

The various experimental points shown in Fig. 3 refer to the same wire and tube system but with the wire pulled through the tube in different directions. The experimental variability of these results was further investigated by repeating the "pull-in" and "pull-out" observations for a second wire-tube assembly, of nominally the same dimensions, after first pulling the wire

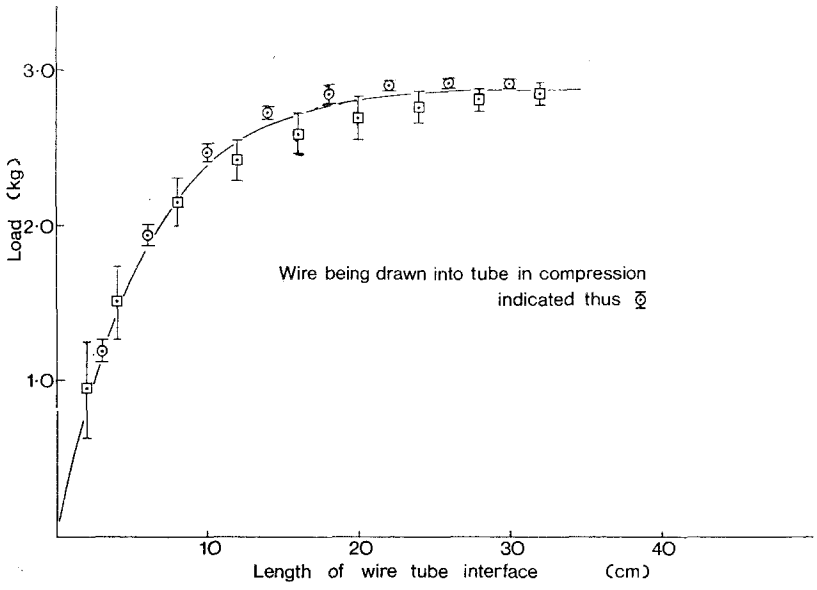

Figure 4 Average values, with 95% confidence limits indicated, for loads required to pull various lengths of convoluted core wire into and out of a tube.

through the tube many times in order to develop a reasonably consistent interfacial condition. These data are shown in Fig. 4 where average load values and 95% confidence limits on the mean values are shown. Data were obtained from four conditions, as the wire was pulled into and out of the tube, with the tube being supported at one end either in tension or compression as this was carried out. The load values obtained as the wire was drawn into the tube when the tube was in compression seemed significantly different from the rest, as is indicated in Fig. 4. The results from the other conditions were, from the available data, indistinguishable and are shown grouped together in Fig. 4.

It seems probable that the reason for the difference noted was due to the slight buckling of the tube which occurs when the wire is drawn into the tube when it is held in compression and is unsupported laterally. This has the effect of increasing the frictional forces and calculations indicate that effects of the same order as those observed could be obtained.

From the experimental values of σ_{max} and the other data given in Fig. 4, and assuming the validity of Equation 6, the numerical value of the constant $2\tau_0/\sigma_{max}\ r$, was calculated for various inserted lengths of convoluted wire. The average value of $2\tau_0/\sigma_{max}\ r$ was then used with Equation 6 to obtain the curve shown in Fig. 4. The value of τ_0 was then calculated, regarding the core-tube interface as being equivalent to the area of the internal surface of the tube, and a value of 0.039 kg mm^{-2} was obtained. The true shear strength of the interface must be much greater than this, however, since the actual area of contact between tube and wire is much less than the internal surface area of the tube. The effective value of τ_0 clearly depends upon the pressure exerted between the wire and the tube, which will depend on the geometry of the system, but is limited by the yield strength of the wire and tube. The value of σ_{max} is also dependent on these factors and this is discussed in Section 2.2.

2.1.2. Core element in compression

When a convoluted wire is pushed into a tube the compressive longitudinal load applied to the wire would tend to increase the amplitude of the convolutions were the wire not restrained by the surrounding tube. As the compressive load is increased there is, therefore, an increasing pressure exerted by the wire on the wall of the tube and hence an increasing frictional force resisting the longitudinal displacement of the core wire within the tube.

The relationship between the shear strength of the frictional interface τ and the tensile stress σ applied to the core wire was assumed to be linear in Equation 3 and this has been shown to be in good agreement with a helically coiled

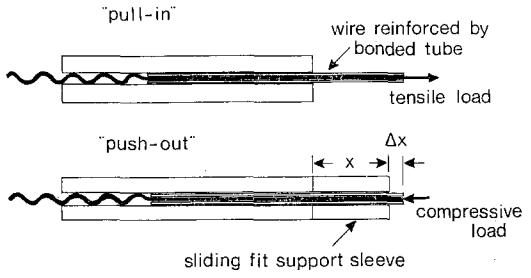

Figure 5 General arrangement of apparatus used to measure the compressive loads required to cause the displacement of various lengths of core wire.

wire/tube arrangement (Figs. 3 and 4). If a linear relationship between τ and σ also holds in compression Equation 6 should describe the compressive stress distribution along a core element loaded at one end, and correspondingly, the stress required to overcome the frictional forces in pushing a given length of core element through a tube.

A simple experimental investigation of this situation has been carried out as illustrated in Fig. 5. A helically coiled wire (system 4 Table I, Section 2.2.2.) was first drawn into a tube for a known distance and the load applied noted. The direction of the applied load was then reversed to push the wire out of the tube and the load required was again noted. During this part of the cycle the wire was prevented from buckling in compression by the supporting tube shown. Successively increasing lengths of core element were drawn into and pushed out of the tube, the applied loads being plotted in Fig. 6. The relationship between the loads applied in compression and tension and the length of wire embedded, x, were then obtained from Equation 6 by substituting L_x and L_{max} for σ_x and σ_{max} where L_x and L_{max} are loads instead of stresses.

$$\text{thus } L_x = L_{max}\,(1 - e^{-Kx})\,. \qquad (7)$$

The value of L_{max} was obtained from the extrapolated experimental data and the curve shown in Fig. 6 was calculated from Equation 7 by taking K as the average of the values computed for each of the experimental points. It is apparent from Fig. 6 that a theoretical curve calculated from an exponential relationship such as described in Equations 6 and 7 is in good agreement with experimental results when the core is loaded either in tension or compression.

2.2. Calculation of theoretical values of σ_{max}

The numerical value of σ_{max} is clearly dependent upon the geometrical form of the convoluted core wire. It is apparent that σ_{max} will become large as the diameter of the core wire approaches the internal diameter of the tube – providing the waveform of the unrestrained wire has an amplitude greater than that of the internal diameter of the tube. Calculations have been

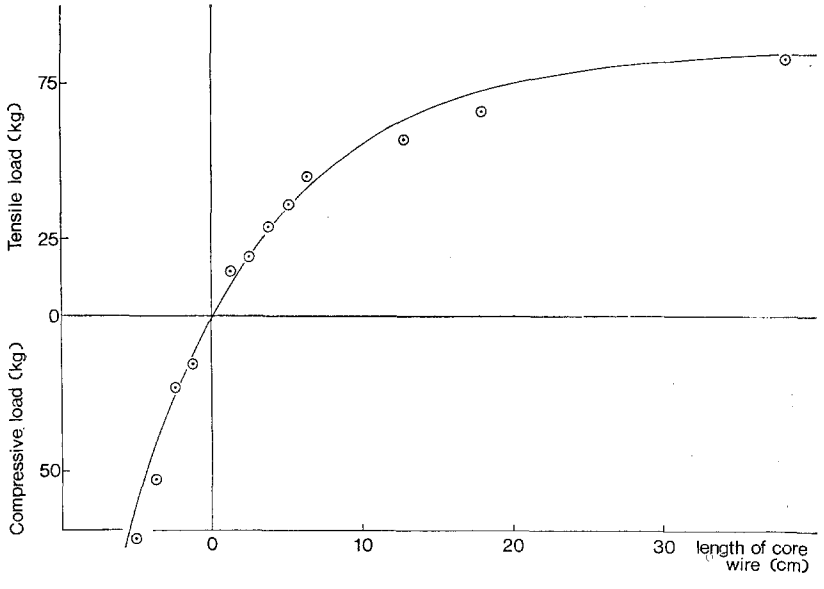

Figure 6 Compressive and tensile loads required to cause the longitudinal displacement of various lengths of core element.

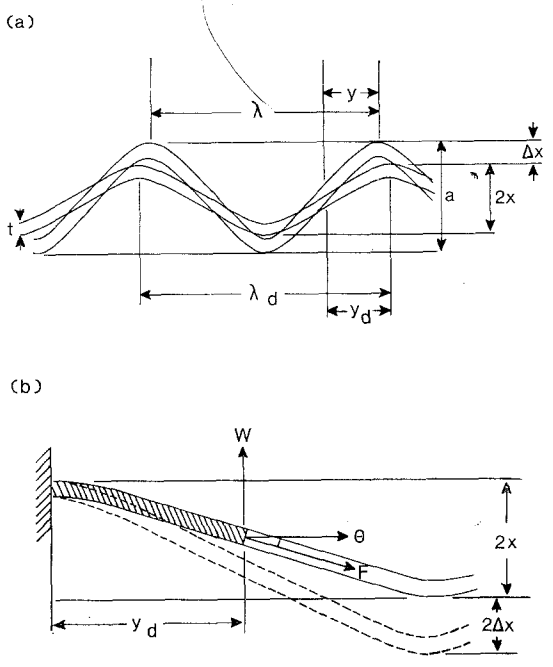

Figure 7 (a) Diagrammatic representation of convoluted strip indicating geometrical measurements made. (b) Equilibrium forces in a convoluted strip.

made of the numerical values of σ_{max} which would be expected with two types of convoluted core element – the first having a sawtooth waveform, the second in the form of a helix. Examples of both arrangements have been examined experimentally and the results obtained compared with the calculated values. The behaviour of both the above systems was nominally elastic. Some preliminary observations were also made of a duplex system in which the core element underwent some plastic deformation during debonding and withdrawal from the surrounding tube.

2.2.1. Sawtooth waveform

For these investigations a model form of variable shear strength interface was produced which consisted of a convoluted spring steel strip compressed elastically between a pair of parallel plates (Fig. 7a). Using this system it was possible to measure directly all the dimensional parameters used to compute values of σ_{max}. Because the amplitude and thickness of the convoluted strip were small compared with its wavelength the force exerted by the strip at the points of contact between it and the parallel plates was calculated by considering each quarter wavelength as a cantilever, encastré at its point of contact with the surface (Fig. 7b).

It follows that the force W exerted by each quarter wavelength of length y is given by

$$W = \frac{3EI\Delta x}{y^3}$$

where E is the Young's modulus of the strip, I is the moment of inertia of its cross-section and Δx is the initial elastic deformation of the strip. Each half wavelength of the strip is in equilibrium when a force W is applied at the "free-end" of the segment, i.e. midway between the plates acting towards and perpendicular to the plates.

Any tensile load carried by the strip can be resolved into components perpendicular to and parallel with the plates. The resolved portion of the tensile load acting perpendicularly to the plates acts in opposition to the force W considered to be acting at the ends of the half wavelength segments. If this force is given by $F \sin \theta$ (where θ is the angle between the strip and the parallel plates), the force exerted by the strip on the plate will be zero when $F \sin \theta + W = 0$. This condition corresponds to σ_{max}.

Now $W = 3EI\Delta x/y^3$ and as F at $\sigma_{max} = \sigma_{max} A$, where A is the cross-sectional area of the strip, we have

$$\sigma_{max} A \sin \theta = \frac{3EI\Delta x}{y^3}.$$

Since $\tan \theta$ is given by $(x - t/2)/y$ where t is the thickness of the strip we have

$$\sigma_{max} = \frac{3EI\Delta x}{y^3 A \sin [\tan^{-1} (x - t/2)/y]}. \quad (8)$$

For small angles of θ, $\sin \theta \simeq \tan \theta$ so that Equation 8 can be written

$$\sigma_{max} = \frac{3EI\Delta x}{y^2 A (x - t/2)}. \quad (9)$$

Equation 8 indicates that σ_{max} will tend to infinity when x approaches a value $t/2$ i.e. when the strip fills the entire space between the plates, providing that Δx has a finite value.

Values of σ_{max} predicted by Equation 8 have been compared with experimental values. These data were obtained from two series of experiments in which the behaviour of a convoluted steel strip (clock spring 0.40 mm thick and 6.26 mm wide and also 0.31 mm × 8.75 mm) mounted between two flat steel plates was observed.

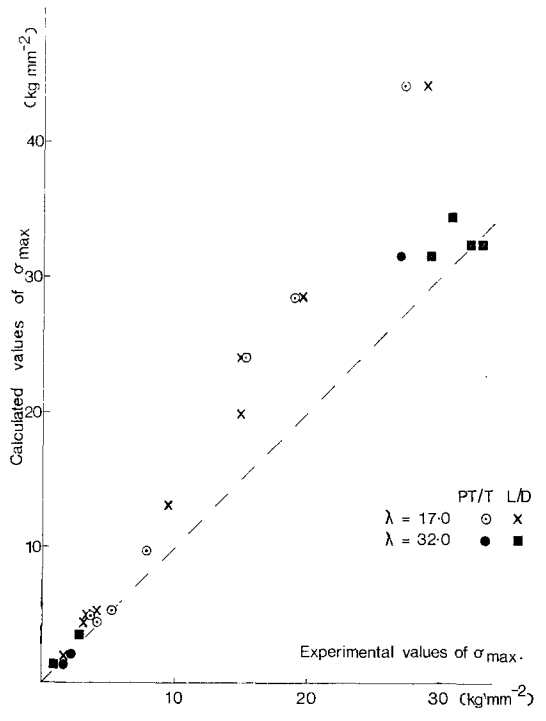

Figure 8 Calculated values of σ_{max} for a convoluted strip compared with experimental values.

In the first series of experiments a convoluted strip was placed between flat steel plates which were then clamped down to fixed spacers so that a frictional force resisting the longitudinal displacement of the strip was generated. The loads required to overcome the frictional forces for various tensile loads applied to the strip were obtained as described in Section 2.1.1. The tensile load carried by the strip, when the force required to withdraw the strip tends to zero, was obtained by extrapolation of the experimental results. The tensile stress in the strip at this point then corresponds to σ_{max}. (*PT/T* values in Fig. 8.)

In the second series of experiments the convoluted steel strips were placed between the plates and the separation of the plates was measured as the tensile load on the strip was varied. From these experimental observations the tensile load required to cause a given convoluted strip to contract laterally to a dimension corresponding to a given separation of the parallel plates could be obtained. This condition again corresponds to the limiting debonding stress σ_{max} for a given geometrical arrangement (*L/D* values in Fig. 8). The wavelength of the convolutions is of course, increased as the amplitude of the waveform is reduced. In Fig. 8 experimental values of σ_{max} obtained by these two techniques for a range of wavelengths, amplitudes and plate separations, are compared with values computed from Equation 8. The observations fall into two groups, one with relatively short wavelength convolutions of about 17 mm, the other with longer wavelengths of about 32 mm. Typical waveforms for these groups are shown in Fig. 9a and b. The longer waveform convolutions correspond fairly closely with the assumptions made in the derivation of Equation 8, and the experimental values of σ_{max} observed for this system agree quite well with the calculated values. In the case of the shorter wavelength system there is a progressively increasing discrepancy between observed and calculated values with increasing values of σ_{max}. The assumptions made in arriving at Equation 8 are clearly not valid for this system.

2.2.2. Helical core

A short length of helix formed from a wire of circular cross-section can be considered as a beam having an initial radius of curvature of ρ_1. When a tensile load is applied to the end of the helix each segment is acted on by a couple which tends to straighten it thus increasing its radius of curvature. If the new radius of curvature is ρ_2 we have

$$M = EI\left(\frac{1}{\rho_1} - \frac{1}{\rho_2}\right)$$

where M is the applied couple, E is the Young's modulus of the material forming the helix, I the moment of inertia of the cross-section of wire forming the helix.

If we assume that the radius of curvature of the helix is the same as that of an ellipse, making the same angle α with a section cut at right angles to the longitudinal axis of the helix, we have from the properties of the ellipse,

$$\rho = \frac{R}{\cos^2 \alpha}$$

where R is the radius of the cylinder upon the surface of which the axis of the wire forming the helix lies. The couple M applied to the helix by a tensile load L is given by

$$LR_2 \sin \alpha_2 = EI\left(\frac{\cos^2 \alpha_1}{R_1} - \frac{\cos^2 \alpha_2}{R_2}\right) \quad (10)$$

where R_1 is the radius of the helix when unstressed, R_2 is the radius of the helix when inside

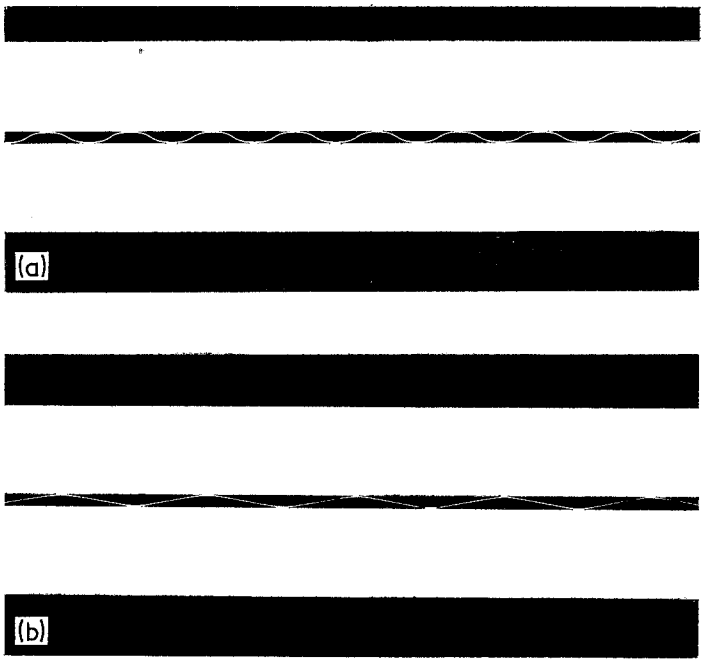

Figure 9 Convoluted steel strip nominal wavelength (a) 17 mm; (b) 32 mm.

the tube, and α_1 and α_2 are the corresponding helix angles. The elastic extension of the wire under load is neglected since this will not affect the wavelength of the helix and will only influence the diameter of the helix through Poisson contraction of the wire.

Four experimental helical core/tube systems have been examined. The helix wires were constructed by first close winding the wire on a mandrel and then stretching it by a suitable amount to produce a helix of the required form. In the case of the samples produced the helix angle, α, lay between 80° and 85°. The wavelength of the helical convolutions, the outside diameter of the helix and the thickness of the wire were measured, and the value of the load required to reduce the initial diameter of the helix to that of the internal diameter of the tube was calculated from Equation 10. This was then compared with the observed limiting load L_{max} required to withdraw a long length of helical core from the tube.

In Table I this comparison is given together with details of the helically coiled wires and tubes used in the experiments. The average internal diameters of the tubes were calculated by weighing the tubes, measuring their lengths and external diameters and assuming a material

TABLE I

	System 1	System 2	System 3	System 4
Wire diameter (mm)	0.26	0.61	0.605	1.07
Wire material	st. steel	st. steel	piano wire	piano wire
Tube internal diameter (mm)	0.419	0.82	0.82	1.48
Diameter of mandrel (mm)	1.99	1.03	1.03	1.99
Free amplitude of helix (mm)	0.5075	0.87	0.865	1.56
Initial wavelength λ (mm)	4.729	6.0	6.045	11.25
Wavelength in the tube λ_2 (mm)	4.761	6.018	6.062	11.27
Initial helix angle α_1	80.65°	82.25°	82.3°	82.14°
Helix angle in tube α_2	83.75°	83.63°	83.7°	83.27°
Youngs modulus of wire (kg mm^{-2})	1.52×10^4	1.52×10^4	2.07×10^4	2.07×10^4
L_{max} calculated (kg)	3.0	24.5	32.8	82.14
L_{max} experimental (kg)	2.9	22.0	30.0	92.85
σ_{max} experimental (kg mm^{-2})	55.0	76.0	104.0	103.25

specific gravity of 7.9. The wire diameters shown are average observed values.

No attempt has been made to allow for local variations in the dimensions of the tubes and wires, but from Table I it is apparent that in the case of the systems studied reasonable agreement exists between the values of L_{max} calculated from Equation 10 and the observed experimental values.

2.2.3. Non-elastic situation

In the conditions discussed above the deformations imposed on the convoluted element were considered to remain within the elastic limit of the material. Characteristics similar to those of elastic systems can, however, be observed when the core element does not remain entirely elastic and where the debonding process results in plastic deformation of the core wire.

Such a system was prepared by crimping steel piano wire of diameter 0.73 mm to form an approximately sinusoidal waveform having a wavelength of 4.117 mm and an amplitude of 0.95 mm. The convoluted wire was then drawn into a steel hypodermic tube having a nominal i.d. of 0.820 mm and an o.d. of 1.065 mm. Because the thickness of the tube wall is relatively small in this system, it was necessary to prevent the tube buckling as the wire was being inserted and this was achieved conveniently by first encapsulating the tube in a polymer block.

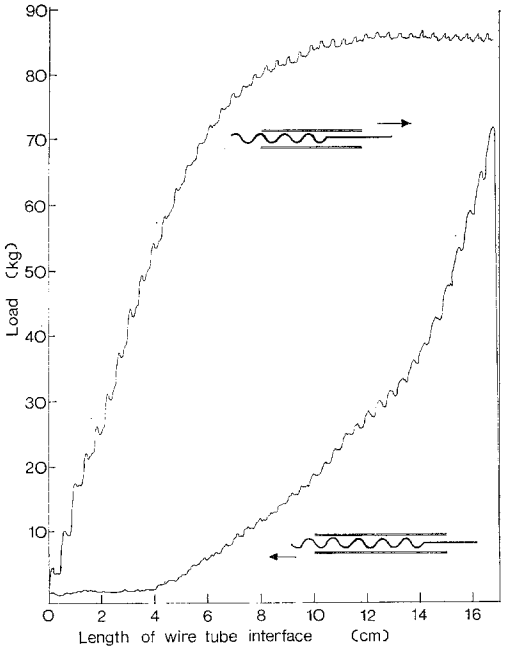

Figure 10 Loads required to pull various lengths of plastically deforming convoluted wire into and out of a close fitting tube.

Tensile stresses approaching 200 kg mm^{-2} have to be applied to the wire in order to draw it into the tube. These stresses are sufficiently high to cause non-elastic straightening of the wire. The load required to pull increasing lengths of wire into the tube is shown in Fig. 10. Also indicated in this diagram are the much smaller loads required to withdraw the wire from the tube in a direction opposite to that of the initial insertion. This is in contrast with the symmetrical distribution observed for the elastic condition shown in Figs. 3 and 4.

If non-elastic core duplex elements are constructed by means other than pulling the core wire into the tube, for example, by drawing down a tube of larger diameter on to a previously inserted core, this asymmetrical condition during initial deformation should be avoidable. The load extension relationship during pull out of the core would then be expected to be similar to the "pull-in" curve, as is the case with the elastic systems.

3. Behaviour of a duplex fibre reinforced composite system in tension

A preliminary study has been made of the deformation and failure in tension of composites consisting of an epoxy resin matrix reinforced with a small number of unidirectionally aligned steel two part duplex reinforcing elements similar to those discussed in Section 2.2.2. The volume fraction of the reinforcing phase was about 10%. Similar specimens containing the same number of unidirectionally aligned wires and tubes were prepared, but in these samples the wires were not placed within the tubes, both wires and tubes being encapsulated individually in the matrix resin.

In all the specimens the resin was notched to initiate failure in the centre of the specimen when stressed in tension in the direction of fibre alignment. In the case of the second configuration, in which both wires and tubes were encapsulated in the resin, failure occurred by the propagation of a single planar crack. Both wires and tubes failed close to the crack surface with little deformation and absorption of energy (Fig. 11a). In the case of the duplex fibre reinforced system a similar failure of matrix and tubes was also observed but the core elements

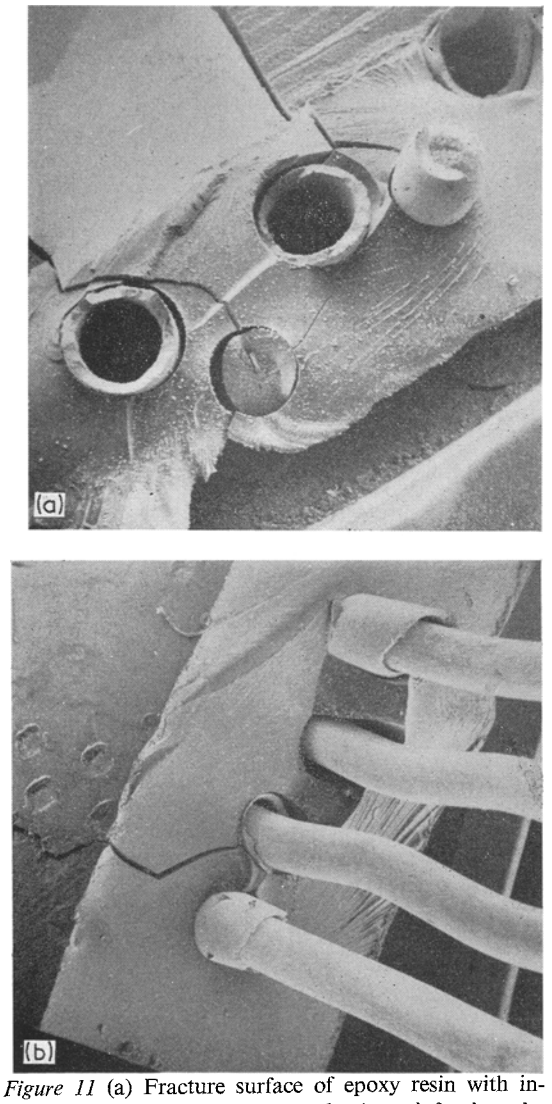

Figure 11 (a) Fracture surface of epoxy resin with individually encapsulated tube and wire reinforcing elements. (b) Fracture surface of epoxy resin with tubes and wires arranged as duplex elements. Wire diameter, 0.73 mm. Tube i.d., 0.825 mm; o.d. 1.06 mm.

were left intact bridging the transverse crack in the composite (Fig. 11b).

For both types of composite the stress required to cause initial failure is largely determined by the stress concentrating ability of the notch. The duplex fibre system continues to carry a load beyond the point of initial failure and the stress level which it can support is controlled by the value of the stress which the core elements carry, and their volume fraction in the composite structure.

The amount of elongation and the overall shape of the load extension curve for the duplex fibre system depends on the specimen length. If the specimen is short compared with the stress transfer length, the stress carried by the core wires at the point of initial failure, can be appreciably less than σ_{max}. However, if the specimen is long compared with the stress transfer length then the core wires carry a stress near to σ_{max} and this does not change appreciably during the early stages of the deformation process. If the reinforcing elements are effectively infinitely long, as is the case for example in a filament wound structure, it would seem that very large "local" tensile extensions will be possible, in the fibre direction, since the core wires can then be pulled considerable distances through the composite structure.

4. Discussion of results and of possible technological applications of duplex fibre composites

4.1. General comments

The experimental observations outlined above demonstrate the feasibility of producing fibrous composites in which the local shear strength of the interface between the reinforcing phase and the rest of the composite structure is controlled by the local tensile stress carried by the reinforcing elements. It has been shown that reinforcing elements of this type can carry high stresses across transverse matrix cracks essentially independent of the overall tensile strain developed in the composite material. Also the core element reinforcing phase is not sensitive to matrix cracks. The experimental work has been solely concerned with steel two-part reinforcing elements used in conjunction with an epoxy resin matrix. However, since the reinforcing elements have been shown to be capable of operating within the elastic range of the material it may prove possible to construct duplex fibres from low density strong brittle elastic materials.

In the case of the particular systems studied the maximum rate of shear stress transfer between core and sheath was of the same order of magnitude (but rather less) than that occurring in glass fibre resin systems, if the area of the interface is assumed to correspond with the surface area of the helical wire. Although higher values may be attainable through an increase in contact pressure and the area of interfacial contact, it would seem unlikely that shear stress transfer values appreciably greater than those found in existing polymer matrix composites will

be attainable by these means. When these relatively low values of shear stress transfer are associated with the use of large diameter elements fairly large stress transfer lengths, perhaps of the order of 10 cm, will be required for the core fibres to develop a large fraction of their maximum load carrying ability. Applications are therefore likely to be limited to large engineering components, particularly filament wound structures, when the maximum contribution by the core to the stiffness and strength of the composite structure is required. These considerations do not necessarily apply where the primary technical requirement hinges on the load limiting and energy absorbing characteristics of the system.

During the course of the experimental work described above, the outer tubular elements have been considered simply as a means to provide a self adjusting shear strength interface between the core element and the rest of the composite structure. Clearly the tubular elements and the outer interface can function as a second reinforcing phase operating largely independently of the core element reinforcing system and the possible advantages of this have been discussed in more detail elsewhere [5]. The tubular elements can contribute to the tensile strength of the composite – up to the point of initial failure – and also to the work of fracture, if a suitable distribution of flaws is provided [6].

4.2. Transverse crack propagation in duplex fibre composites

In present day fibrous composites the interfacial characteristics are normally arranged so that a propagating matrix crack does not cause immediate failure of the fibres and they are left intact bridging the crack tip. Such fibres will fail if their failing strain is exceeded. In the case of the stress controlled reinforcing systems described above, the fibres can remain intact bridging the entire length of a matrix crack despite large separations of the crack faces.

Observations have been made [7, 8], of the work of fracture of a thin metal plate reinforced with a small volume fraction of reinforcing elements of this type. The crack was propagated by a crack opening force applied at the mouth of the crack and the work of fracture was found to increase with increasing crack length. Very high specific energy absorption values (energy absorbed per unit cross-sectional area of core elements) were observed when the matrix crack reached an appreciable size.

When a reinforced plate of this type is subjected to a uniform stress applied in the direction of fibre alignment there are two general conditions to consider. If the stress carried by the reinforcing elements approaches σ_{max} then the elements are effectively decoupled from the composite structure and their only effect is to reduce the load which would otherwise be carried by the plate. If, however, during crack propagation in the plate, the stress carried by the reinforcing element is less than σ_{max} there will be an interaction between the plate and the reinforcing phase. This can have two effects. If any differential movement occurs between the plate and the crack bridging reinforcing elements, then energy will be dissipated by frictional effects. At the same time the reinforcing phase tends to restrain the plate from relaxing as much as it would otherwise have done in the absence of the crack bridging reinforcing elements. The effect of this is to reduce the amount of strain energy available to propagate the crack and to provide an additional mechanism by which strain energy is absorbed compared with the unreinforced condition [9].

Acknowledgement

The work reported here forms part of a basic study of composite materials which is supported by the Science Research Council and the Wolfson Institute of Interfacial Technology.

References

1. L. J. BROUTMAN and R. H. KROCK (eds), "Modern Composite Materials" (Addison Wesley, Reading, Mass. and London, 1967) Chapter 2.
2. J. O. OUTWATER JUN, *Mod. Plast.* **33** (1956) 156.
3. A. KELLY, "Strong Solids" (Clarendon Press, Oxford, 1966) Chapter V, p. 139.
4. A. H. COTTRELL, *Proc. Roy. Soc. London* **A282** (1963) 1. See also A. KELLY, *ibid* **A319** (1970) 95.
5. J. G. MORLEY, *ibid* **A319** (1970) 117.
6. G. A. COOPER, *J. Mater. Sci.* **5** (1970) 645.
7. J. G. MORLEY, Faraday Society Special Discussion Meeting, Solid-Solid Interface (1972).
8. *Idem*, paper 47 in the Mictrostructure and Design of Alloys, Proceedings of the 3rd International Conference on the Strength of Metals and Alloys (1973) Institute of Metals and the Iron and Steel Institute.
9. J. G. MORLEY and I. MCCOLL, to be published.

Received 5 February and accepted 8 February 1974.